

International Journal of Modern Physics E
 © World Scientific Publishing Company

PROBING EFFECTIVE NUCLEON-NUCLEON INTERACTION AT BAND TERMINATION

W. SATULA*

*Institute of Theoretical Physics, University of Warsaw,
 ul. Hoża 69, 00-681 Warsaw, Poland,*

Received (received date)

Revised (revised date)

Low-energy nuclear structure is not sensitive enough to resolve fine details of nucleon-nucleon (NN) interaction. Insensitivity of infrared physics to the details of short-range strong interaction allows for consistent, free of ultraviolet divergences, formulation of local theory at the level of local energy density functional (LEDf) including, on the same footing, both particle-hole as well as particle-particle channels. Major difficulty is related to parameterization of the nuclear LEDf and its density dependence. It is argued that structural simplicity of terminating or isomeric states offers invaluable source of informations that can be used for fine-tuning of the NN interaction in general and the nuclear LEDf parameters in particular. Practical applications of terminating states at the level of LEDf and nuclear shell-model are discussed.

1. Introduction

The atomic nuclei are very complex finite many-body systems exhibiting non-trivial coupling of single-particle (sp) and collective degrees of freedom. It is well known that significant fraction of these many-body correlations can be taken into account through symmetry violating intrinsic states within self-consistent mean-field (MF) approximation using finite-range Gogny¹ or contact Skyrme² interactions. These interactions, or the underlying energy density functionals (EDF), are parametrized usually by about ten coupling constants which are adjusted to basic properties of nuclear matter and to selected data on finite nuclei.

The fitting procedure is by no means unambiguous. There is no clear consensus of what dataset should be used in adjusting EDF parameters. Coupling between single-particle and collective degrees of freedom and correlations beyond MF manifestly appearing in any finite mesoscopic system implies further that different philosophy (procedures and datasets) should, in principle, be applied while fitting EDF for pure MF applications and for theoretical methods taking explicitly correlations beyond MF approximation like random phase approximation, generator-coordinate

*satula@fuw.edu.pl

method, or symmetry-projection techniques to avoid double counting. Yet another open problem is related to density dependence of nuclear EDF coupling constants and its relation to the NNN interaction. Presently used prescription is purely phenomenological. It is not only unsatisfactory from theoretical point of view but cause numerous troubles in particular in angular momentum projected calculations, see ³ and refs. quoted therein. Similar ambiguities related to the form and density dependence apply to pairing channel.

The number of existing parameterizations of, in particular, Skyrme forces reflects ambiguities listed above. This rather frustrating situation can be healed to a certain extent by turning the attention to specific, extremely simple nuclear states where pairing, single-particle and collective degrees of freedom decouple to the largest possible extent. The classical examples of such states are superdeformed states or terminating and high-spin isomeric states, see ^{4,5} and refs. cited therein.

Hereafter I will focus on applications of terminating and high-spin isomeric states. The aim is to demonstrate how the structural simplicity of these states can be used to probe nuclear Skyrme EDF (see Ref. ^{6,7} for further details), pairing correlations as well as effective *sdfp* shell-model (SM) NN interaction.

I will start by presenting general arguments speaking in favor of local nuclear theory. I will show next a couple of numerical results pertaining to isovector pairing correlations. In particular, I will consider three versions of density dependent delta interaction (DDDI) including volume-active, surface-active and mixed variants. I will present examples of calculated shape-gap correlation plots that seem to quite firmly point out toward volume-like character of nucleonic isovector pair field by excluding both surface-active or mixed pairing scenarios. Next, I will briefly overview problems with conventional pair-blocking encountered in the analysis of $N=83$ high-spin isomeric states in rare-earth nuclei. Finally, I will discuss the energy differences between two terminating configurations $[f_{7/2}^n]_{I_{max}}$ and $[d_{3/2}^{-1}f_{7/2}^{n+1}]_{I_{max}}$ in $Z \leq N$, $A \sim 45$ mass region

$$\Delta E = E([d_{3/2}^{-1}f_{7/2}^{n+1}]_{I_{max}}) - E([f_{7/2}^n]_{I_{max}}). \quad (1)$$

This extremely simple observable can be used not only to test time-odd spin-fields and spin-orbit strength of the nuclear EDF ^{6,7} but also elucidates much more subtle effects directly pertaining to isospin dependence of SM matrix elements.

2. Infrared nuclear theory

2.1. Particle-hole channel

Nuclear structure theory aims to describe low-energy nuclear excitations. Since such observables are by definition not sensitive enough to resolve details of the underlying NN (and NNN) interaction one can freely relax any less or more stringent relation between effective and *ab initio* NN (and NNN) potentials and attempt to build the effective nuclear theory essentially from scratch using, as the only guiding principle, the following general statement: *low-energy or INFRARED physics*

should not depend on high-energy or ULTRAVIOLET dynamics. Such separation of scales is the underlying principle of effective field theory which aims to describe composite objects at low-energies by Lagrangians which include ultraviolet dynamics by means of a series of contact corrections⁸. It implies that the following expansion of an arbitrary short-range, rotationally invariant NN interaction:

$$v_S(q^2) \approx v_S(0) + v_S^{(1)}(0)q^2 + v_S^{(2)}(0)q^4 \dots, \quad (2)$$

in terms of transferred momentum q should converge fast.^a In this way complicated and in fact unknown two-body NN interaction is mapped by just a few constants: $v_S(0), v_S^{(1)}(0), \dots$ which should be carefully adjusted using representative set of nuclear data.

In the r -space the expansion (2) takes the following form

$$\begin{aligned} v_{eff}(\mathbf{r}) \approx & v_{long}(\mathbf{r}) \\ & + ca^2\delta_a(\mathbf{r}) \\ & + d_1a^4\nabla^2\delta_a(\mathbf{r}) + d_2a^4\nabla\delta_a(\mathbf{r})\nabla \\ & + \dots \\ & + g_1a^{n+2}\nabla^n\delta_a(\mathbf{r}) + \dots, \end{aligned} \quad (3)$$

where $\delta_a(\mathbf{r})$ denotes an arbitrary model of the Dirac delta function of range a . The $v_{long}(\mathbf{r})$ describes the long-range part of the NN potential. Since typical range of strong interaction is $a \sim 1$ fm and is much smaller than nuclear radius R , $a \ll R$, the $v_{long}(\mathbf{r})$ pertains essentially to Coulomb interaction. The correcting terms are proportional to $\delta_a(\mathbf{r})$ and derivatives of $\delta_a(\mathbf{r})$ arranged as in Eq. (3) to assure spherical symmetry. Each correcting term introduces its own dimensionless coupling constant $c, d_1, d_2 \dots g_1 \dots$ since the effective range $\sim a$ or ultraviolet cut-off momentum $\sim 1/a$ is pulled out explicitly in Eq. (3). As already mentioned these coupling constants should be readjusted to a selected set of low-energy data.

The assumed spherical symmetry defines uniquely (Eq. (3)) the form of the correcting potential replacing the low-momentum part of the exact potential removed by the ultraviolet cut-off procedure. However, since $\delta_a(\mathbf{r})$ can be modeled in essentially arbitrary way, there is, at least in principle, an infinite set of equivalent realizations of the effective interactions or effective theories. In particular, assuming Gaussian form factor:

$$\delta_a(\mathbf{r}) \equiv \frac{e^{-\mathbf{r}^2/2a^2}}{(2\pi)^{3/2}a^3}, \quad (4)$$

or more precisely modeling $\delta_a(\mathbf{r})$ by a sum of attractive and repulsive Gaussians of different ranges with space-, spin- and isospin-exchange term and supplementing it by a density dependent term and a spin-orbit term (last two terms in Eq. (5))

^aAt this stage we omit, for the sake of simplicity, spin and isospin degrees of freedom.

4 *W. Satula*

leads to the Gogny force ¹

$$\begin{aligned}
 v(1, 2) = & \sum_{j=1}^2 e^{r_{12}^2/\mu_j^2} \left(W_j - B_j \hat{P}_\sigma - H_j \hat{P}_\tau - M_j \hat{P}_\sigma \hat{P}_\tau \right) \\
 & + t_3 (1 + x_3 \hat{P}_\sigma) \rho_0^\gamma(\mathbf{R}) \delta(\mathbf{r}_{12}) \\
 & + i W_0 (\boldsymbol{\sigma}_1 + \boldsymbol{\sigma}_2) \left(\hat{\mathbf{k}}' \times \delta(\mathbf{r}_{12}) \hat{\mathbf{k}} \right) .
 \end{aligned} \tag{5}$$

Since the early work of Brink and Vautherin ⁹ it is known that particle-hole (ph) channel can be described by contact $\lim_{a \rightarrow 0} \delta_a = \delta(\mathbf{r})$ Skyrme interaction ²:

$$\begin{aligned}
 v(1, 2) = & t_0 (1 + x_0 \hat{P}_\sigma) \delta(\mathbf{r}_{12}) \\
 & + \frac{1}{2} t_1 (1 + x_1 \hat{P}_\sigma) \left(\hat{\mathbf{k}}'^2 \delta(\mathbf{r}_{12}) + \delta(\mathbf{r}_{12}) \hat{\mathbf{k}}^2 \right) \\
 & + t_2 (1 + x_2 \hat{P}_\sigma) \hat{\mathbf{k}}' \delta(\mathbf{r}_{12}) \hat{\mathbf{k}} \\
 & + \frac{1}{6} t_3 (1 + x_3 \hat{P}_\sigma) \rho_0^\gamma(\mathbf{R}) \delta(\mathbf{r}_{12}) \\
 & + i W_0 (\boldsymbol{\sigma}_1 + \boldsymbol{\sigma}_2) \left(\hat{\mathbf{k}}' \times \delta(\mathbf{r}_{12}) \hat{\mathbf{k}} \right) ,
 \end{aligned} \tag{6}$$

where: $\mathbf{r}_{12} = \mathbf{r}_1 - \mathbf{r}_2$; $\mathbf{R} = (\mathbf{r}_1 + \mathbf{r}_2)/2$; the momentum operator $\hat{\mathbf{k}} = \frac{1}{2i}(\nabla_1 - \nabla_2)$ acts to the right while $\hat{\mathbf{k}}' = -\frac{1}{2i}(\nabla_1 - \nabla_2)$ acts to the left hand side. The first three terms of the Skyrme interaction correspond to the first three terms in the expansion (3). Last two terms in Eq. (6) denote density dependent and spin-orbit terms.

The concept of effective theory based on renormalization of ultraviolet dynamics turns up side down the philosophy behind the effective NN forces. It states that due to *poor* resolution of low-energy data the exact form of the NN force is not at all needed in practical computations. It can be replaced by local corrections of the form given in Eq. (3). The insensitivity of the effective theory to the short-range details tells us that we can construct infinitely many theories having the same low-energy behavior. All of them (although different and having probably not much in common with the true short-range part of the NN interaction) are essentially equivalent in the sense that all of them should be capable to reproduce low-energy nuclear data with desired accuracy when order-by-order refinement (3) is applied. In this sense Gogny and Skyrme interactions appear as two independent (among infinitely many) realizations of an effective theory. So far, Skyrme interaction was viewed rather as a short-range expansion of finite-range Gaussian force ⁹ and regarded as a limiting case of a seemingly more fundamental finite-range Gogny force.

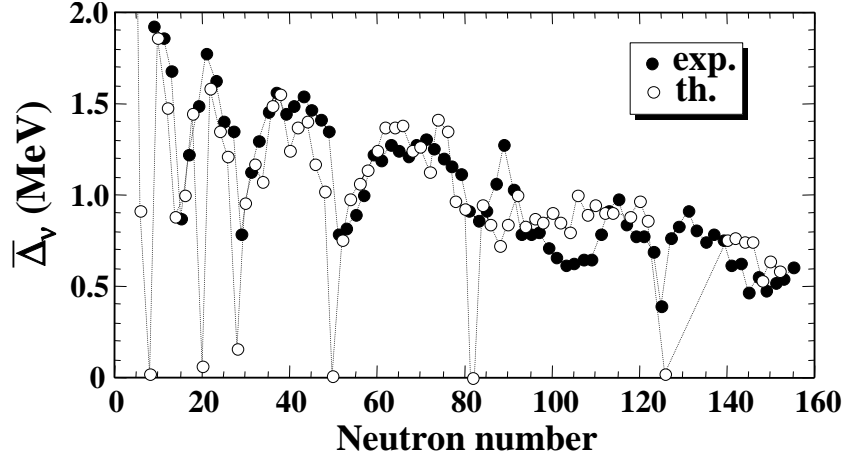


Fig. 1. Mean neutron pair gaps calculated using HFB D1S Gogny method (open dots) in Ref. ¹⁰ in comparison to empirical three-point OES data $\Delta(\text{odd} - N)$ (filled dots).

2.2. Particle-particle channel

The particle-hole and particle-particle (pp) or pairing interactions can be treated independently. One can therefore apply similar expansion to the pp interaction:

$$v_{\text{pair}}(q^2) \approx g + g_2 q^2 + g_4 q^4 \dots \quad (7)$$

By retaining only the first term in (7) and by modeling it by a Gaussian-type Dirac-delta model (4) one obtains finite range Gogny pairing force which appeared to be very successful in numerous practical applications. The example of such calculations illustrating Hartree-Fock-Bogolyubov (HFB) mean neutron gap calculated using D1S Gogny force versus neutron number ¹⁰ is shown in Fig. 1. Note, that the theoretical pair-gaps follow very closely empirical three-point odd-even staggering (OES) data:

$$\Delta(N) = \frac{(-1)^N}{2} [B(N-1) + B(N+1) - 2B(N)], \quad (8)$$

extracted for odd- N nuclei which, in accordance with the analysis of Refs. ^{11,12}, represents mean pair gap. In particular no low-mass enhancement of the pair gap following conventional textbook $\Delta \sim 1/\sqrt{A}$ estimate is seen neither in the data nor in the calculations. An additional advantage of finite-range pairing model is that it automatically removes high-momentum scattering processes. Indeed, due to the finite-range r_o ($r_o \sim 1$ fm) the Gogny force discriminates states above $E_c \sim p_c^2/2m_r \sim \hbar^2/mr_o \sim 40$ MeV [$m_r = m/2$ is reduced mass] since $r_o p_c \sim \hbar$.

In spite of its success the use of finite range interaction in the pp channel may be viewed as rather unnecessary complication. Indeed, in the nuclear matter pairing

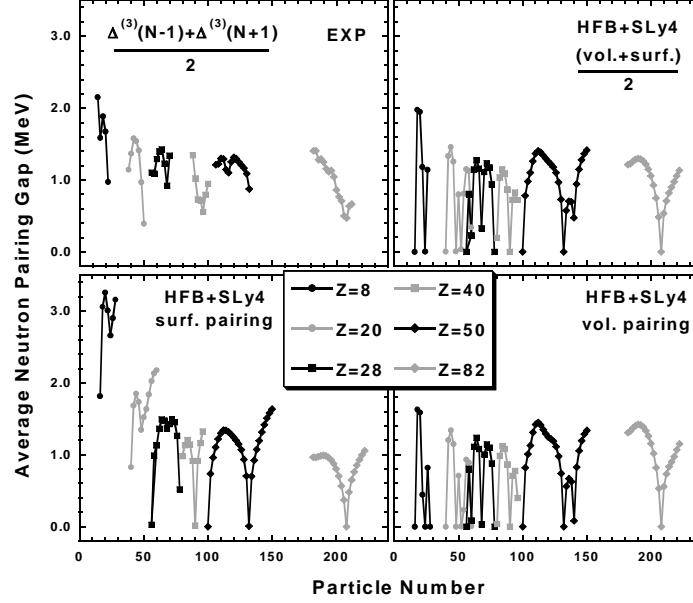


Fig. 2. Neutron pair-gaps versus neutron number. Upper left panel shows empirical OES. The remaining panels illustrate pair-gaps obtained within Skyrme-HFB model using three different versions of the DDDI interaction: surface-active (lower left), mixed (upper right) and volume-active (lower right). Taken from Ref. ¹³.

modifies the nucleonic motion essentially only in the closest vicinity of the Fermi energy, $E_F - \Delta \leq \frac{(p_F \pm \delta p)^2}{2m} \leq E_F + \Delta$ giving rise to uncertainty in momentum space, $\delta p \sim \Delta/v_F$. This uncertainty translates to uncertainty in coordinate space $\xi \sim \frac{(\hbar c)^2 k_F}{(mc^2)\Delta} \gg r_o \sim \frac{1}{k_F}$ which by far exceeds the typical interaction range r_o . Consequently, the nucleonic Cooper pairs appear as spatially extended objects which can hardly feel subtle details of the underlying NN pairing interaction. Nuclear pairing should be therefore well described within local approximation using plain delta interaction or, slightly more general, density dependent delta interaction (DDDI):

$$v_{pair}(\mathbf{r}) = v_o \left[1 - \left(\frac{\rho(\mathbf{r})}{\rho_c} \right)^\alpha \right] \delta(\mathbf{r}). \quad (9)$$

We are again touching a subtle question of resolution and sensitivity of low energy data but this time with respect to pairing. In particular case of nuclear matter it was demonstrated explicitly by Garrido *et al.* ¹⁴ that one can rather easily parametrize interaction (9) in order to reproduce pair-gap $\Delta(k_F)$ versus k_F dependence in nuclear matter (with free particle spectrum) obtained using Gogny interaction. In the case of finite nuclei the situation is far more complicated. Figure 2 illustrates empirical neutron-gap (OES) and the results of large scale spherical

Skyrme-HFB calculations using DDDI interaction in pp channel¹³. Three different versions of the calculations are depicted corresponding to surface ($\rho_c = \rho_o$), mixed ($\rho_c = 2\rho_o$) and volume ($\rho_c \rightarrow \infty$) type pairing scenarios. In all cases $\alpha = 1$. The strength v_o was adjusted separately for each pairing-mode in order to reproduce empirical neutron pair-gap in ^{120}Sn .

The overall agreement between neutron OES and the calculated pair-gaps is satisfactory for volume-active and mixed pairing scenarios. For these two pairing scenarios the agreement is also similar to the one obtained with Gogny-pairing shown in Fig. 1. Clearly, the OES itself is not *sensitive* enough to differentiate neither between these two variants of the DDDI interaction nor between the DDDI and Gogny pairing. On the other hand the calculations clearly prefer volume or mixed DDDI over pure surface-active DDDI. Indeed, the surface-active pairing leads to enhanced neutron gaps in light systems which are not at all observed in the data.

Further inside into a character of nuclear pairing can be gained by looking into correlation plots of deformation, which is rather robust observable, versus pairing gap. An example of such shape-gap consistency plot is shown in Fig. 3. Two different examples of rather well deformed nuclei are depicted in the figure. Left part shows β_2 -vs- Δ_n plot in ^{50}Cr . This is a typical case when shape-gap consistency between calculations and the data (marked by the area where horizontal and vertical shaded areas corresponding to empirical uncertainties in β_2 and Δ_n cross each other) can be reached essentially irrelevant of the assumed pairing scenario. Hence, this example shows *no sensitivity* at all with respect to the considered pairing variant. The right hand side of Fig. 3 shows similar β_2 -vs- Δ_n plot but for ^{46}Ti . In this case shape-gap consistency requirement simply *excludes* both the surface-active and mixed pairing scenarios. There are at least two almost obvious questions which need to be answered in this context: (i) Can the hierarchy of deformed-to-spherical phase transition versus pairing type which so clearly seen in Fig. 3 be understood in a simple manner? (ii) Is the case exclusiveness in ^{46}Ti accidental or it can be traced down systematically throughout the periodic table? Studies along these lines are under way.

2.3. Toward consistent superfluid local density approximation

The disadvantage of using DDDI type (local) pairing interaction as compared to finite-range Gogny interaction is that the former requires explicit cutoff parameters to avoid divergences. In particular, all Skyrme-HFB calculations presented above were done within limited phase-space for pairing. Although practically sufficient in most applications, such a brute-force method is unsatisfactory from theoretical point of view. In this respect, local pairing can be considered as considerably disadvantageous as compared to finite-range pairing. It appears however, that the divergence can be rather easily identified and subsequently regularized leading to consistent cutoff-free superfluid local density approximation (SLDA)^{15,16}.

The appropriate scheme for regularization of ultraviolet divergence in anomalous

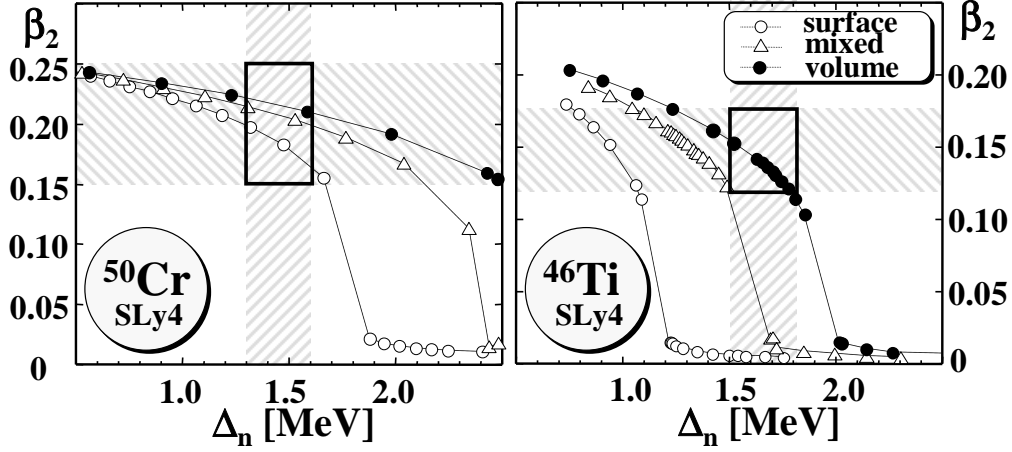
8 *W. Satula*

Fig. 3. Shape-gap correlation plot in ^{50}Cr (left) and ^{46}Ti (right). Three different curves represent Skyrme-HFB calculations assuming surface-active (open dots), mixed (triangles) and volume-active (black dots) pairing variants.

density matrix:

$$\nu(\mathbf{r}_1, \mathbf{r}_2) = \sum_i v_i^*(\mathbf{r}_1) u_i(\mathbf{r}_2) \sim \frac{1}{|\mathbf{r}_1 - \mathbf{r}_2|}, \quad (10)$$

at the level of the local density approximation (LDA) i.e. including properly dominant particle-hole channel was recently proposed by Bulgac and Yu¹⁶. The idea is to renormalize divergent terms by introducing cutoff ($E_c \equiv \frac{(\hbar k_c)^2}{2m}$) dependent counter-terms. Such an approach leads to standard local HFB formalism with cut-off parameters but with a gap equation dependent on the effective *running* coupling constant:

$$\nu_c(\mathbf{r}) = \sum_{E_i \geq 0}^{E_c} v_i^*(\mathbf{r}) u_i(\mathbf{r}), \quad (11)$$

$$\Delta(\mathbf{r}) = -g_{eff}(\mathbf{r}) \nu_c(\mathbf{r}), \quad (12)$$

$$\frac{1}{g_{eff}(\mathbf{r})} = \frac{1}{g[\rho(\mathbf{r})]} - \frac{m(\mathbf{r}) k_c(\mathbf{r})}{2\pi^2 \hbar^2} \left\{ 1 - \frac{k_F(\mathbf{r})}{2k_c(\mathbf{r})} \ln \frac{k_c(\mathbf{r}) + k_F(\mathbf{r})}{k_c(\mathbf{r}) - k_F(\mathbf{r})} \right\}. \quad (13)$$

Introducing a *running* coupling constant implies that the cutoff dependence is only formal and disappears for sufficiently large E_c ¹⁶. The cutoff-free superfluid LDA approach is now in phase of extensive tests^{16,17}.

3. Pairing in high-spin isomeric states

The atomic ground states are strongly correlated. Simple mean-field-plus-pairing model, although quite successful in reproducing nuclear masses, see Ref.¹⁸ and refs.

cited therein, cannot incorporate all important correlations and polarization effects within single symmetry-broken Slater determinant. Hence, in order to test/tune less ambiguously basic theoretical ingredients of our models it seems natural to change the attitude and look not into terribly complicated strongly correlated states but turn the attention toward as pure as possible physical situations.

The high-spin isomeric states (HSI) open new and so far not fully explored possibilities to study, in particular, pair correlations, blocking phenomena and superfluid-to-normal phase transition^{19,20}. They are structurally extremely simple hence both configuration and shape can be kept rather well under control in the calculations. In turn, shape and pairing polarization due to blocking can be studied in detail. As an example let us recall systematic calculations by Xu *et al.*²¹ who, using HSI, re-examined traditional average gap method²² used to determine monopole pairing strength G_{MN} for Lipkin-Nogami calculations. In particular, it was found that inclusion of polarization effects requires $\sim 10\%$ larger pairing strength G_{MN} as compared to the average-gap value²¹ in order to reproduce experimental data.

Recently the HSI have been systematically observed in $N=83$ nuclei with $60 \leq Z \leq 67$ ²³. In odd-A nuclei the HSI have $J^\pi=49/2^+$ and correspond to a seniority-five, stretched shell-model configuration $[C_o: \nu(f_{7/2}h_{9/2}i_{13/2}) \otimes \pi h_{11/2}^2]_{49/2}^+$. In odd-odd nuclei the observed HSI have $J^\pi=27^+$ and are assigned to $[C_{oo}: \nu(f_{7/2}h_{9/2}i_{13/2}) \otimes \pi(d_{5/2}^{-1}h_{11/2}^2)]_{27}^+$ configuration. These two configurations differ by a single proton hole in Nilsson $[402]5/2$ orbital originating from spherical $d_{5/2}$ sub-shell. This unique data set enables to study for the first time OES both at the ground states (GS) as well as at high-spins using conventional technique based on binding energy indicators²⁴. The most striking feature of this data set is an almost constant excitation energy of the HSI what implies that OES at the ground states (GS) follows very closely the HSI value $\Delta_{GS}(Z) \approx \Delta_{HSI}(Z)$. Conventional interpretation of this empirical result in terms of pairing-gap suggests the lack of blocking phenomenon. Note, that this conclusion is independent on the type of pairing indicator. Hence, in the following, we will use standard three-point filter $\Delta(Z)$ (see^{11,12} for detailed discussion of its physical content) of Eq. (8).

The importance of pair-correlations at the HSI can be elucidated by considering extreme single-particle model. An example of such calculations is shown in Fig. 4. The figure compares experimental OES of Eq. (8) to theoretical OES computed using self-consistent SHF model with SLy4²⁵ and SkO²⁶ parameterizations. The theoretical values show clear systematic rise not at all observed in the data. This theoretical trend is generic and reflects the fact that, within the extreme sp scenario, the indicator (8) measures simply a distance between proton Fermi energy e_F and proton hole state $e_{[402]5/2}$ as indicated in the right hand side of the figure. The increase of $\Delta(Z)$ with Z is therefore generic to any sp model. It can be naturally stopped (or slowed down) when ph excitations are replaced by quasi-particle excitations i.e. in the presence of relatively strong pair-correlations.

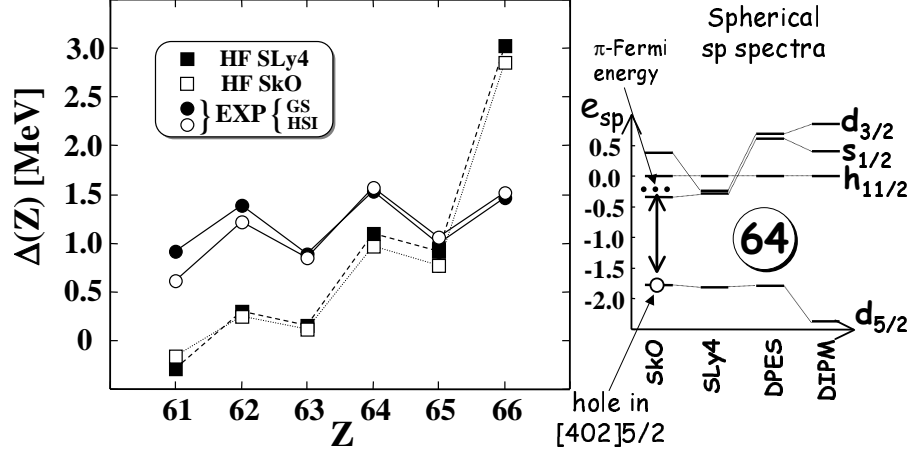


Fig. 4. Experimental (dots) and theoretical (squares) OES of Eq. (8). Calculations for fixed configurations C_o and C_{oo} were carried out with single-particle SHF-SLy4 and SHF-SkO models. Right hand side shows spherical single-particle spectra of all models discussed in the context of HSI normalized to $h_{11/2}$. This part of the figure illustrates schematically a dominant within the sp scenario and increasing with Z contribution to OES, $\Delta(Z) \sim e_F - e_{[402]5/2}$, originating from energy difference between "fixed in energy" proton hole $[402]5/2$ and proton Fermi energy which is "moving up" in energy with increasing Z .

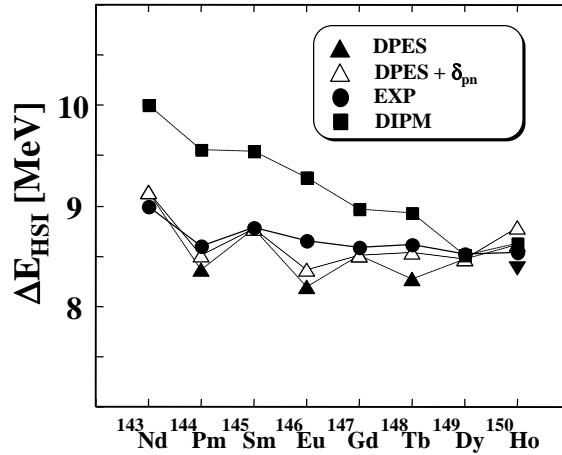


Fig. 5. Experimental (filled circles) and theoretical (DIPM: squares; DPES: triangles) excitation energies of HSI in the $N=83$ isotones. Open triangles show the DPES calculations corrected by the pn residual interaction δ_{pn} extracted from nuclear binding energies using the 9-point indicator of Ref. ²⁴.

To study pairing properties of GS and HSI states we employed two different approaches: the deformed independent particle model (DIPM) ²⁷ and the diabatic

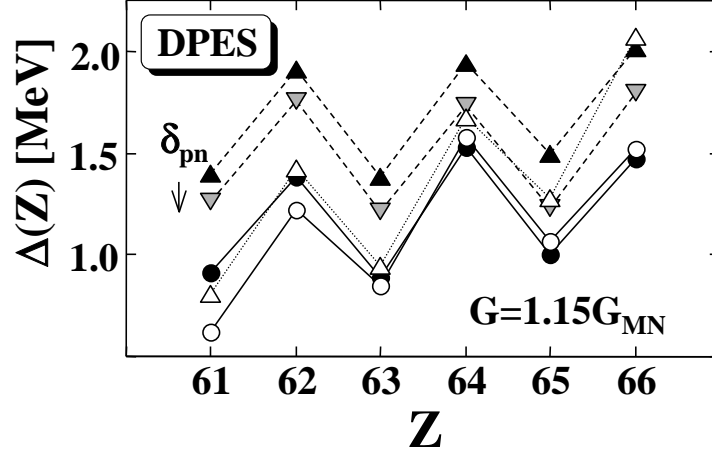


Fig. 6. $\Delta(Z)$ of Eq. (8) calculated using DPES model. Filled (open) symbols denote GS (HSI) values. The effect of δ_{pn} on GS DPES values is indicated (gray triangles). Experimental values of $\Delta(Z)$ are marked by dots.

potential energy surface model (DPES)²⁰. For the $N=83$ isotones, both DIPM and DPES methods yield fairly consistent results. Namely, both methods predict: (i) weakly deformed ground states; (ii) well-deformed, oblate ($\beta_2 \approx -0.2$) HSI states (iii) C_o and C_{oo} yrast HSI configurations. The only exception is ^{150}Ho where DPES predicts the C_{oo} configuration to lie ~ 150 keV above the HSI configuration involving four aligned $h_{11/2}$ protons. The calculated excitation energies of HSI, ΔE_{HSI} , slightly depend on the model used reflecting mostly the differences in sp spectra of the underlying mean-potentials, see Fig. 4 and Fig. 5. Note, that agreement between DPES prediction and experimental ΔE_{HSI} is excellent particularly after correcting theoretical results for residual neutron-proton interaction present in the GS of odd-odd nuclei. Further details concerning both the models and results can be found in²³.

The OES of Eq. (8) calculated using the DPES model is shown in Fig. 6. The values calculated at the HSI follow experimental data very closely meaning that our theoretical tools and/or interactions can be very reliably tuned out in such simple situations. On the other hand, the theory faces serious troubles in reproducing OES in the GS. The complexity of GS causes that contributions to OES due to pairing, sp-proton energy splitting, residual proton-neutron (pn) interaction and/or nuclear magnetism (time-odd effects) which must all be taken into account simultaneously in order to reproduce experimental data are difficult to control in a satisfactory way in strongly correlated states. In particular, our calculations clearly indicate that contribution due to blocking which is mainly responsible for shift of theoretical GS and HSI curves in Fig. 6 is far too strong and requires revisiting.

4. Probing isospin dependence of SM matrix elements at band termination.

Recently, it was shown ⁶ that a set of terminating states in the mass region $A \sim 45$ may provide a unique tool to constrain the Skyrme energy density functional (SEDF). The key idea is to look into energy differences (1) between two types of terminating configurations $[f_{7/2}^n]_{I_{max}}$ and $[d_{3/2}^{-1}f_{7/2}^{n+1}]_{I_{max}}$ i.e. into the quantity which, as the long experience in the studies of terminating states within the Nils-son model have clearly shown, see Ref. ^{4,5} and refs. quoted therein, belong to the purest single-particle observables available in nuclear structure. In particular, it was demonstrated ⁶ that by constraining the SEDF to the empirical spin-isospin Landau parameters and by slightly reducing the spin-orbit strength, good agreement with the data could be obtained. This result, based on high-spin data for terminating states, is consistent with conclusions of previous works ^{28,29} based on different theoretical methodology and experimental input (such as giant resonances, beta decays, and moments of inertia). The validation of the assumption ⁶ regarding the single-particle character of the maximally-aligned states and the robustness of terminating states in determining properties of the nuclear EDF was further supported by the recent comparative study between the fully correlated shell model (SM) and the Skyrme Hartree-Fock (SHF) ³⁰, showing essentially a one to one correspondence between the models at least for $N > Z$ nuclei, see Fig. 7.

In the $N=Z$ nuclei the comparison between the models can be done only after evaluation of the correlation energy δE_T due to the spontaneous breaking of isobaric symmetry in the SHF. The correction due to isospin symmetry restoration shifts the $T=0$ state down in energy in the laboratory system, as illustrated in the inset of Fig. 7. After (phenomenological) symmetry restoration predictions from both SM and SHF models become very similar in all considered nuclei. However, while the agreement in $N > Z$ is satisfactory the $N=Z$ results deviate strongly from the data. Definitely too strongly as compared, in particular, to overall excellent performance of the fp shell SM ³¹.

One possible origin of this deviation may have its source in the assumed truncation to 1p-1h cross-shell excitations. This configuration-space restriction is expected to impact the isoscalar channel associated with the $sd \rightarrow fp$ pair scattering i.e. isoscalar proton-neutron pairing (pn) mode which is also absent in conventional mean-field description. A possibility of an onset of the isoscalar pn pairing nearby band-termination was already discussed within the mean-field formalism in Ref. ³².

An alternative source of deviation may be traced back to incorrect isospin dependence of SM matrix elements. The quantity (1) involves particle-hole excitation. In such a case, according to Bansal and French ³³, and Zamick ³⁴ (BFZ) ... *it is a grave error to assume that ph interaction is independent on isotopic spin....* Under certain assumptions listed in Refs. ^{33,34} the isotopic dependence of ph interaction can be approximated by a simple monopole interaction $\sim bt_1 \cdot t_2$ yielding additional

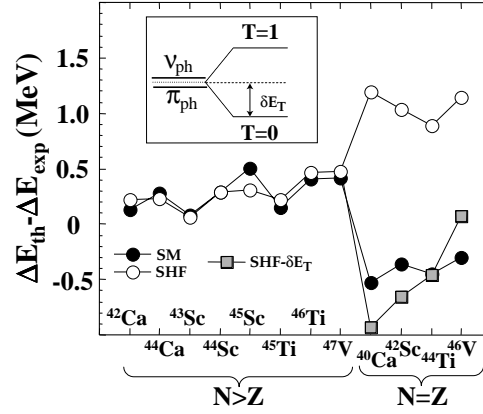


Fig. 7. Difference $\Delta E_{th} - \Delta E_{exp}$ between experimental and theoretical values of ΔE (1) in $A \sim 44$ mass region. Dots denote the SM results. Circles denote the SHF results based on the modified SkO parameterization (see text). The SHF calculations for the $[d_{3/2}^{-1} f_{7/2}^{n+1}]_{I_{max}}$ intruders in $N=Z$ nuclei yield two nearly degenerate states associated with proton (π_{ph}) and neutron (ν_{ph}) cross-shell excitations. As shown in the inset, the physical $T=0$ state in the laboratory frame is shifted down in energy by δE_T (isospin correlation energy). Squares denote the SHF results for $N=Z$ nuclei with the isospin correction added. The SHF results were shifted by 480 keV in order to facilitate the comparison with SM. Taken from Ref. ³⁰.

contribution to ΔE of Eq. (1) of the form:

$$\Delta E^T = \frac{1}{2}b(T(T+1) - T_p(T_p+1) - T_h(T_h+1)), \quad (14)$$

where $T_h = 1/2$ and $T_p = T \pm 1/2$ are hole and particle contributions to the isotopic spin T . In the case of terminating states in $N=Z$ nuclei $T_p = 1/2$ while for terminating states in $N > Z$ we have $T_p = T - 1/2$. Hence, the anticipated contributions to the ΔE due to the BFZ mechanism are:

$$\Delta E^T = \begin{cases} -\frac{3}{4}b & \text{in } N = Z \\ \frac{1}{2}b\left(T - \frac{1}{2}\right) & \text{in } N \neq Z \end{cases} \quad (15)$$

If, for some reason, the strength of the monopole interaction b is overestimated in the SM by $\delta b = 700$ keV (in this mass region it amounts to $\delta b/b \sim 20\%$) the SM values of ΔE should be corrected by: 525 keV in $N=Z$ nuclei; 0 keV in $T = 1/2$ ^{43}Sc , ^{45}Ti , and ^{47}V nuclei; -175 keV in $T = 1$ ^{42}Ca , ^{44}Sc and ^{46}Ti nuclei; -350 keV in $T = 3/2$ nucleus ^{45}Sc ; -525 keV in $T = 2$ nucleus ^{44}Ca . The corrected values are depicted in Fig. 8. Note that they match empirical the data almost perfectly.

The suggestion that the discrepancy between the SM description of $N > Z$ and $N = Z$ nuclei may be caused (fully or partly) by incorrect isospin dependence of

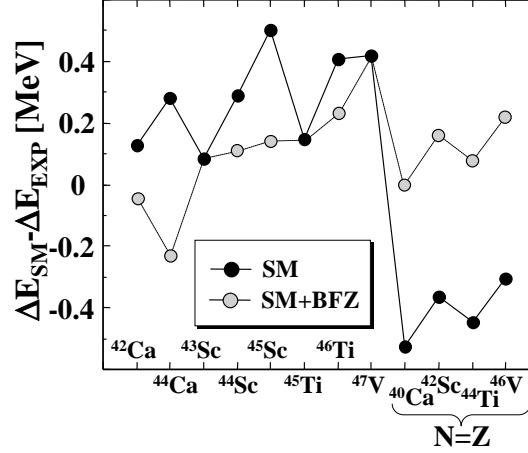


Fig. 8. The differences $\Delta E_{SM} - \Delta E_{EXP}$ calculated using SM model (black dots). Grey dots indicate SM values corrected by the anticipated contributions due to BFZ effect of Eq. (15), assuming $\delta b = 700$ keV decrease in the b strength.

the SM matrix elements ^{35,36} is extremely intriguing and the anticipated accuracy of $\Delta E_{SM} - \Delta E_{EXP}$ deduced solely on the basis of the BFZ formula is indeed very appealing, see Fig. 8. To verify the concept we performed two set of SM calculations using modified SM interactions marked lateron as SM⁽¹⁾ and SM⁽²⁾, respectively.

In the SM⁽¹⁾ run ALL diagonal particle-hole matrix elements of original SM interaction ^{35,36} were renormalized according to the following scheme:

$$\begin{aligned} V_{phph}(JT=0) &\rightarrow V_{phph}(JT=0) + 3d \\ V_{phph}(JT=1) &\rightarrow V_{phph}(JT=1) - d \end{aligned} \quad (16)$$

with $d = 0.175$ keV. The use of transformation (16) can be partly justified within single j -shell shell-model phenomenological mass formula where it appears to leave invariant all contributions to the binding energy except the symmetry energy strength b_{sym} which changes according to the following rule: $b_{sym} \rightarrow b_{sym} - 4d$, see Ref. ³⁷. It should be underlined, however, that b and b_{sym} although having certain common features are different quantities. Such an attempt to modify b was not fully successful and satisfactory. On one side we obtained substantial improvement of agreement to the data for low-lying particle-hole excitations as compared to the original interaction as shown in Fig. 9. On the other side the changes appeared not neutral with respect to other observables spoiling, in particular, the previously obtained nice agreement between SM and experimental binding energies.

In the SM⁽²⁾ run we have decided to apply renormalization scheme (16) to CROSS-SHELL matrix elements only. Preliminary calculations shows that such a simple procedure leads to an almost perfect agreement between theory and experiment for both terminating as well as low-lying particle-hole excitations. Further

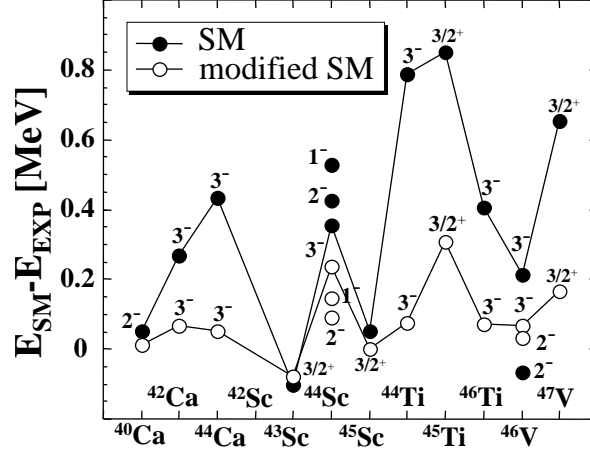


Fig. 9. Difference between the SM and experimental excitation energies for selected low-spin 1p-1h intruder states. Calculations done using original SM interaction (bullets) are compared to the results obtained for modified SM⁽¹⁾ interaction. Note dramatic improvement obtained for modified SM.

details concerning our systematic refinements of SM interaction inspired by very precise high-spin data including both sets of modifications discussed above will be published elsewhere ³⁸.

5. Summary and outlook

It is shown, that local effective theory suitable for low-energy nuclear structure calculations can be consistently formulated as free form ultraviolet divergences superfluid local energy density functional approach. The underlying assumption concerning independence of infrared physics on ultraviolet dynamics implies that such a strictly local theory should in principle be equivalent to finite-range effective theory concerning accuracy of its predictions. This conclusion makes local realization of effective theory extremely appealing due to its numerical simplicity.

There are at least two major problems related to the nuclear LEDF including: (i) Density dependence of LEDF parameters or coupling constants and its relation to effective three body NNN interaction. This problem pertains both to local as well as to finite-range nuclear EDF formalism in the same way. (ii) Datasets used to parametrize are definitely incomplete leading to a multitude of local (Skyrme) effective interactions. In this respect finite-range realizations of effective theories are less prone to the details of datasets as our practice with the Gogny interaction shows where essentially only two parameterizations are used in numerical applications ³⁹. This is related with smaller number of terms that are used in the expansion (3).

The relations between the LEDF parameters and fine-tuning of the LEDF parameters can be reliably done in simple physical situations. Long standing experi-

ence tells that terminating or isomeric states belong to the purest known examples of almost unperturbed single-particle motion ⁴. In this work we summarize our recent efforts related to terminating and isomeric states showing, in particular, that:

- The structural simplicity of these states can be used to unify time-odd spin-fields and tune up spin-orbit strength of the LEDF, see ^{6,30} for further details.
- They can be used for identification, evaluation and subsequent restoration of broken symmetries inherently obscuring the SHF treatment, see Ref. ^{30,?} for further details.
- Multi quasi-particle configurations in rare-earth nuclei can be used to test pairing interaction and blocking phenomena ²³.
- Finally, it is shown that these states appear to be extremely useful in identifying and correcting isobaric dependence of cross-shell matrix elements of *sdpf* SM interaction ^{30,38}.

6. Acknowledgments

The results presented in this manuscript are due to common effort of many colleagues. I would like to acknowledge cordially very fruitful collaboration with D. Dean, M. Kosmulski, W. Nazarewicz, H. Sagawa, G. Stoitchewa, R.A. Wyss, M. Zalewski, and H. Zduńczuk. This work has been supported in part by the Polish Committee for Scientific Research (KBN) under Contract No. 1 P03B 059 27.

References

1. D. Gogny, *Proc. Int. Conf. on Nuclear Physics*, eds. J. De Boer and H. Mang (North-Holland, Amsterdam, 1973; *Nuclear Self-Consistent Fields*, ed. G. Ripka and M. Porneuf (North-Holland, Amsterdam, 1975) p. 333.
2. T.H.R. Skyrme, *Phil. Mag.* **1** (1956) 1043; *Nucl. Phys.* **9** (1959) 615.
3. M. Bender, these proceedings; L.M. Robledo, *ibid.*; H. Zduńczuk, W. Satuła, and J. Dobaczewski, *ibid.*
4. A.V. Afanasjev *et al.*, *Phys. Rep.* **322** (1999) 1.
5. W. Satuła and R. Wyss, *Rep. Prog. Phys.* **68** (2005) 131.
6. H. Zduńczuk, W. Satuła, and R. Wyss, *Phys. Rev.* **C58** (2005) 024305; *Int. J. Mod. Phys.* **E14** (2005) 451; W. Satuła, R. Wyss, and H. Zduńczuk, *Eur. Phys. J. A* **25**, s01, (2005) 551. .
7. M. Zalewski *et al.*, submitted to *Phys. Rev. C* (2006); M. Zalewski and W. Satuła, these proceedings.
8. G.P. Lapage, nucl-th/9706029; U. van Kolck, *Prog. Part. Nucl. Phys.* **43** (1999) 337; S.R. Beane *et al.*, nucl-th/0008064.
9. D. Vautherin and D.M. Brink, *Phys. Rev.* **C5** (1972) 626.
10. S. Hilaire *et al.*, *Phys. Lett.* **B531** (2002) 61.
11. W. Satuła, J. Dobaczewski, and W. Nazarewicz, *Phys. Rev. Lett.* **81** 3599 (1998).
12. J. Dobaczewski *et al.* *Phys. Rev.* **C63** (2001) 024308.
13. J. Dobaczewski, W. Nazarewicz, and M. Stoitsov, in *The Nuclear Many-Body problem 2001*, eds. W. Nazarewicz and D. Vretenar, Kluwer Academic Publishers, 2002, p. 181; J. Dobaczewski and W. Nazarewicz, *Prog. of Theor. Phys. Suppl.* No **146**, (2002).

14. E. Garrido *et al.*, Phys. Rev. **C60** (1999) 064312.
15. T. Papenbrock and G.F. Bertsch, Phys. Rev. **C59** (1999) 2052.
16. A. Bulgac, Phys. Rev. **C65** (2002) 051305; A. Bulgac and Yongle Yu, Phys. Rev. Lett. **88** (2002) 042504; Int. J. Mod. Phys. **E13** (2004) 147.
17. P.J. Borycki *et al.*, Phys. Rev. **C73**, 044319 (2006).
18. D. Lunney, J.M. Pearson, and C. Thibault, Rev. Mod. Phys. **75** (2003) 1021.
19. G.D. Dracoulis, F.G. Kondev, and P.M. Walker, Phys. Lett. **B419** (1998) 7.
20. F.R. Xu *et al.*, Phys. Lett. **B435** (1998) 257.
21. F.R. Xu, R. Wyss, and P.M. Walker, Phys. Rev. **C60** (1999) 051301.
22. P. Möller and J.R. Nix, Nucl. Phys. **A536** (1992) 20.
23. A. Odahara *et al.*, Phys. Rev. **C72** (2005) 061303(R).
24. A.S. Jensen *et al.*, Nucl. Phys. **A431** (1984) 393.
25. E. Chabanat, *et al.*, Nucl. Phys. **A627** (1997) 710; **A635** (1998) 231.
26. P.-G. Reinhard *et al.*, Phys. Rev. **C60** (1999) 014316.
27. T. Døssing *et al.*, Phys. Scr. **24**, 258 (1981).
28. F. Osterfeld, Rev. Mod. Phys. **64** (1992) 491.
29. M. Bender *et al.*, Phys. Rev. **C65** (2002) 054322.
30. G. Stoitcheva *et al.*, Phys. Rev. **C73** (2006) 061304(R).
31. E. Caurier *et al.*, Rev. Mod. Phys. **77** (2005) 427.
32. J. Terasaki, R. Wyss, and P.-H. Heenen, Phys. Lett. **B437** (1998) 1.
33. R.K. Bansal and J.B. French, Phys. Lett. **11** (1964) 145.
34. L. Zamick, Phys. Lett. **19** (1965) 580.
35. W.A. Richter *et al.*, Nucl. Phys. **A523** (1991) 325.
36. E.K. Warburton, J.A. Becker, and B.A. Brown, Phys. Rev. **C41** (1990) 1147.
37. N. Zeldes, in *Handbook of Nuclear Properties*, Ed. by D. Poenaru and W. Greiner, Clarendon Press, Oxford, 1996, p. 13.
38. G. Stoitcheva, W. Satuła, and W. Nazarewicz, in preparation.
39. J. Dechargé and D. Gogny, Phys. Rev. **C21** (1980) 1568; J.-F. Berger, M. Girod, and D. Gogny, Nucl. Phys. **A428** (1984) 23c.